The EMBO Journal vol.14 no.19 pp.4641–4653, 1995

# Altered T cell development in mice with a targeted mutation of the CD3-ε gene

**Marie Malissen, Anne Gillet, Laurence Ardouin, Gaelle Bouvier, Jeannine Trucy, Pierre Ferrier, Eric Vivier and Bernard Malissen[1]**

Centre d'Immunologie INSERM-CNRS de Marseille-Luminy, Case 906, 13288 Marseille Cedex 9, France

[1]Corresponding author

**To determine which CD3 components are required for early T cell development, we generated mice with a targeted mutation of the CD3-ε gene and characterized their T cell populations relative to those found in CD3-ζ/η- and recombinase activating gene (RAG)-deficient mice. In the absence of intact CD3-ε subunit, thymocytes do not progress beyond the CD44$^{-/low}$CD25$^{+}$ triple-negative stage and appear to be arrested at the very same developmental control point as RAG-deficient thymocytes. In contrast, the disruption of the CD3-ζ/η gene does not totally abrogate the progression through this control point. CD3-ε-deficient thymocytes do rearrange their T cell receptor (TCR) β gene segments and produce low levels of full-length TCR β transcripts. Taken together, these results establish an essential role for the CD3-ε gene products during T cell development and further suggest that the CD3-ε polypeptides start to exert their function as part of a pre-TCR through which CD44$^{-/low}$CD25$^{+}$ triple-negative cells monitor the occurrence of productive TCR β gene rearrangements. Finally, the absence of intact CD3-ε polypeptides had no discernible effect on the completion of TCR γ and TCR δ gene rearrangements, emphasizing that they are probably not subjected to the same epigenetic controls as those operating on the expression of TCR α and β genes.**

*Keywords*: gene targeting/gene rearrangements/T cell development/T cell receptor–CD3 complex

## Introduction

T cells can be divided into two subsets based on the structure of their T cell antigen receptor (TCR). In the adult, most T cells express a TCR heterodimer consisting of α and β chains, whereas a minor population expresses an alternative TCR made of γ and δ chains. Each of these four TCR chains includes a clonally variable (V) region. During intrathymic development, the genes encoding the TCR V regions are assembled via a series of site-specific DNA recombinations. β chain V genes are formed through random recombination of single elements selected from among three discrete libraries of gene segments (or sub-exons) denoted variable (Vβ), diversity (Dβ) and joining (Jβ). Likewise, α chain V genes are assembled randomly from two separate libraries of gene segments called variable (Vα) and joining (Jα). During V→J, V→D or D→J recombination, coding gene segment ends are generally subjected to varying degrees of base deletion, addition, or both, before ligation (Lewis, 1994). As a consequence, V(D)J joining events could result either in productive rearrangements that maintain an open reading frame throughout the gene, or in out-of-frame, non-productive rearrangements.

The most immature cells identified in the adult thymus are present in small numbers (~0.2% of all thymocytes) and bear low levels of CD4, Thy1 and heat-stable antigen (HSA), and high levels of CD44 and stem cell factor receptor (c-kit) (Wu *et al.*, 1991; Godfrey *et al.*, 1994). They carry their TCR loci in germline configuration and may develop along the αβ or γδ T cell lineages following intrathymic transfer. During the initial step of maturation, these 'CD4$^{low}$ precursors' up-regulate Thy1 and HSA and lose CD4 to become 'triple-negative' (CD4$^{-}$CD8$^{-}$CD3$^{-}$) cells. This heterogeneous population of triple-negative cells comprises 2–4% of total thymocytes. Their differentiation is marked by the transient expression of the interleukin-2 receptor α chain (CD25) and the loss of both CD44 and c-kit expression. The late triple-negative cells can progress to the CD4$^{+}$CD8$^{+}$ ('double-positive') stage via intermediates which express either CD4 or CD8 in the absence of mature αβ TCR and are therefore called 'immature single-positive' cells. A small percentage of the double-positive cells further mature into CD4$^{+}$CD8$^{-}$ or CD4$^{-}$CD8$^{+}$ ('mature single-positive') cells that correspond to the end products of the intrathymic αβ T cell differentiation pathway.

Analysis of the intrathymic reconstitution potential, cell cycle status and TCR gene configuration of the early T cell subsets found in the adult thymus allowed the following maturation sequence to be deduced: CD4$^{low}$CD8$^{-}$ CD44$^{+}$CD25$^{-}$c-kit$^{+}$ → CD4$^{-}$CD8$^{-}$CD3$^{-}$CD44$^{+}$CD25$^{+}$c-kit$^{+}$ → CD4$^{-}$CD8$^{-}$CD3$^{-}$ CD44$^{-/low}$CD25$^{+}$c-kit$^{-/low}$ → CD4$^{-}$CD8$^{-}$CD3$^{-}$ CD44$^{-/low}$CD25$^{-}$c-kit$^{-}$ (reviewed in Godfrey and Zlotnik, 1993). TCR β gene rearrangements precede rearrangements at the TCR α locus and start at, or at the transition to, the CD44$^{-/low}$CD25$^{+}$ triple-negative stage. They proceed in two separately controlled steps involving an initial D→J joining event and a subsequent V→DJ rearrangement. The CD44$^{-/low}$CD25$^{+}$ population corresponds to a continuum of cells in the process of TCR β rearrangement, of which many have yet to complete V→ DJ joinings (Levelt *et al.* 1993a; Dudley *et al.*, 1994). In contrast, the next two developmental stages (CD44$^{-/low}$CD25$^{-}$ and immature single-positive), display a pattern of TCR β transcripts which resembles that found in mature T cell populations, suggesting that TCR β rearrangements are essentially completed at these stages (Godfrey *et al.*, 1994; Wilson *et al.*, 1994). The first TCR

α rearrangements, as inferred from the presence of 1.6 kb TCR α transcripts, are detectable during or immediately after the transition to the double-positive stage (A.Wilson, personal communication).

When they rearrange their TCR genes non-productively or express TCR αβ combinations with inappropriate specificities, thymocytes are generally arrested at one of two discrete developmental control points. Checkpoints have evolved to ensure that the transition through these control points is coupled to the attainment of certain landmark events in T cell development. One checkpoint for T cell maturation controls the transition from the double-positive to the single-positive stage (a phenotypic shift often denoted as positive selection) and its activation depends on both the ligand specificity of the clonally variable TCR αβ dimer and the efficiency of the selection process (reviewed in Kisielow and von Boehmer, 1995). The other checkpoint occurs earlier in development and controls the transition from the $CD44^{-/low}CD25^{+}$ to the $CD44^{-/low}CD25^{-}$ triple-negative stage. A host of experiments suggests that this checkpoint is activated upon TCR β chain expression. For instance, the thymocytes found in mice deficient in at least one of the two V(D)J recombinase-activating genes (RAG-1 or RAG-2) are unable to rearrange their TCR genes and are blocked at the $CD44^{-/low}CD25^{+}$ triple-negative stage. Complementation of these mutant mice with a productively rearranged TCR β chain (but not α chain) transgene restores a normal developmental progression (encompassing CD25 down-regulation, induction of CD4 and CD8 expression, as well as cellular expansion) which ends up at the double-positive stage and brings the absolute number of double-positive cells in the wild-type range (Mombaerts *et al.*, 1992; Shinkai *et al.*, 1993; Shinkai and Alt, 1994). In the absence of TCR α chain (not yet expressed at the $CD44^{-/low}CD25^{+}$ stage), the TCR β chain covalently associates with a surrogate pre-TCR α (pTα) chain which is encoded by a non-rearranging gene (Saint-Ruf *et al.*, 1994). The resulting pTα–TCR β heterodimers combine with CD3 subunits to form a pre-TCR complex through which $CD44^{-/low}CD25^{+}$ cells presumably monitor productive TCR β gene rearrangements (Levelt *et al.*, 1993b; Dudley *et al.*, 1994). The identity of the CD3 chains present within such pre-TCR complexes remains controversial. While CD3-ε and CD3-γ have been found repeatedly associated with the pre-TCR complexes expressed in pre-T cell lines and early thymocytes, CD3-ζ and CD3-δ have been more difficult to detect and may therefore be only loosely or not associated with it (Punt *et al.*, 1991; Groettrup *et al.*, 1992; Shinkai *et al.*, 1993; Jacobs *et al.*, 1994). The requirement for TCR β chain expression in the progression to the double-positive stage can be overcome in RAG-deficient mice by the injection of anti-CD3-ε monoclonal antibodies. (Levelt *et al.*, 1993b; Jacobs *et al.*, 1994; Shinkai and Alt, 1994). Therefore, under physiological conditions, the pre-TCR complex is likely to signal via its CD3 subunits; the role of pTα being so far unclear. Considering that the CD3 and pTα subunits are already expressed at the $CD44^{-/low}CD25^{+}$ stage and do not constitute rate-limiting factors (Saint-Ruf *et al.*, 1994; Wilson and MacDonald, 1995), the pre-TCR complex is likely to constitute a multimolecular sensor, the assembly and inducing function of which are totally coupled to the achievement of a productive TCR β chain gene rearrangement. To identify which CD3 components are required for early T cell development to proceed, we have generated mice with a targeted mutation of the CD3-ε gene and characterized their T cell populations relative to those found in RAG- and CD3-ζ/η-deficient mice.

## Results

### *Targeting of the CD3-ε gene*

The mouse CD3-ε gene contains eight exons and gives rise to a polypeptide of 21–26 kDa (Clevers *et al.*, 1988). The construct pRH20A used for targeting the CD3-ε gene was designed to insert a pgk–neo cassette in place of exon 5 which codes for most of the CD3-ε extracellular domain (Figure 1A). The linearized targeting vector was electroporated into the Bruce 4 embryonic stem (ES) cell line. Clones resistant to both neomycin and gancyclovir were screened by Southern blotting for homologous recombination events. Two homologous recombinants were identified out of 192 colonies tested. Germline transmission was obtained with one clone, and homozygous mutant mice were generated by intercrosses of heterozygous mice. To determine whether CD3-ε mRNAs were produced in mice homozygous for the mutation, we analyzed total RNA derived from thymocytes by Northern blotting (Figure 2). After hybridization to a CD3-ε probe, the homozygote mutant thymocytes (Figure 2, lane $CD3\text{-}\varepsilon^{\Delta5/\Delta5}$) were found to express a very faint band at ~1.3 kb, whereas the wild-type, $RAG\text{-}1^{-/-}$ and $CD3\text{-}\zeta/\eta^{-/-}$ thymocytes each contained high levels of the expected 1.5 kb CD3-ε mRNA. To confirm that a truncated CD3-ε transcript was being produced at low levels in the mutant cells, a pair of primers specific for transcripts initiating at the CD3-ε promoter was used to amplify, by PCR, cDNA synthesized from total thymocyte RNA. As shown in Figure 1B, intact CD3-ε mRNAs (507 bp) were produced only in the wild-type and heterozygote mutant mice. Interestingly, the latter also contained a weaker band which corresponded in size (291 bp) to transcripts expected to result from skipping of exon 5. Comparison of wild-type and homozygote mutant mice showed that these shorter transcripts originated from the targeted CD3-ε allele. Moreover, the relative intensity of the two hybridizing bands detected in the heterozygotes under conditions of template competition indicated that the truncated mRNAs originating from the mutant CD3-ε allele were much less abundant than the wild-type CD3-ε mRNAs. These results prompted us to test for the presence of truncated CD3-ε polypeptides in the homozygote mutant thymocytes. When analyzed by Western blot and probed with a rabbit antiserum directed against a peptide corresponding to the cytoplasmic C-terminal end of CD3-ε, thymocyte lysates from homozygote mutant mice were found to contain truncated CD3-ε polypeptides migrating at a position corresponding to the one predicted for CD3-ε proteins devoid of the extracellular domain normally encoded by exon 5 (~13 kDa, Figure 1C, lane $CD3\text{-}\varepsilon^{\Delta5/\Delta5}$). Quantification of the bands shown in Figure 1C indicated that the amount of truncated CD3-ε polypeptides in the homozygous mutant cells corresponded to $<1\%$ of the full-length CD3-ε polypeptide observed in wild-type thymocytes. Therefore, these data indicate that the targeted CD3-ε allele, which we will

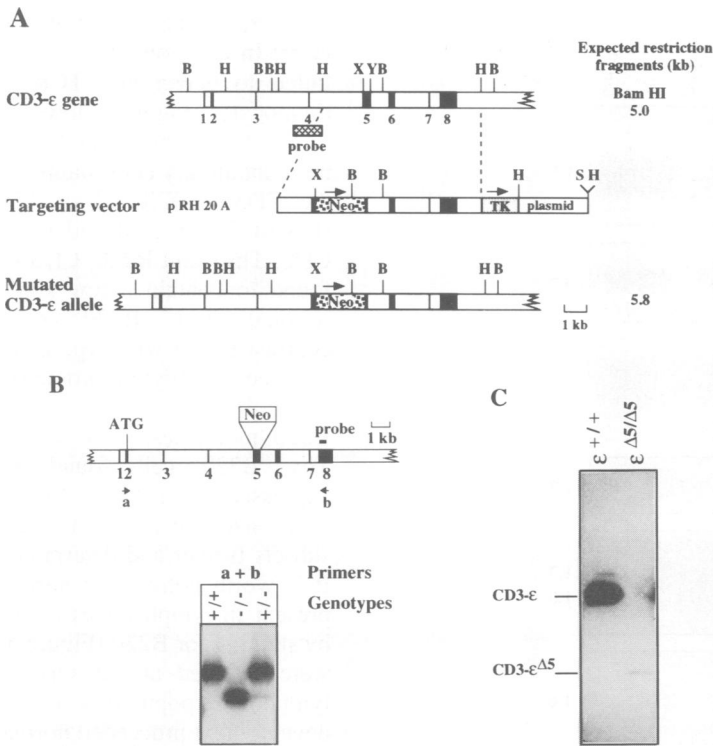


**Fig. 1.** Construction and characterization of the CD3-ε targeted mice. (**A**) Disruption of exon 5 of the CD3-ε gene by homologous recombination. The first line shows the exon–intron organization of the mouse CD3-ε gene according to Clevers *et al.* (1988). Exons are depicted as filled boxes and numbered 1–8. The targeting construct (pRH20A) used to disrupt the CD3-ε gene corresponds to a 6.5 kb *Hin*dIII fragment into which a pgk–neo cassette (*neo*) has been inserted within exon 5. The insertion of the *neo* cassette was accompanied by the deletion of a 168 bp fragment coding for most of exon 5. The resulting construct was abutted to a TK expression cassette (TK) and electroporated into ES cells. The structure of the disrupted gene is indicated on the bottom line. Homologous recombinants were confirmed by restriction enzyme digestion and Southern blot analysis using a 1.2 kb *Hin*dIII–*Kpn*I genomic fragment as a probe. This probe, the position of which is shown below the CD3-ε gene (probe), hybridizes on *Bam*HI-digested DNA to a 5.0 kb wild-type fragment and to a 5.8 kb recombinant fragment. Horizontal arrows above the *neo* and TK genes indicate 5′→3′ orientation. The positions of relevant restriction sites are indicated by vertical lines: B, *Bam*HI; H, *Hin*dIII; S, *Sal*I; X, *Xba*I and Y, *Xho*I. (**B**) Analysis of CD3-ε transcripts by RNA-PCR in thymus from wild-type, heterozygote and homozygote mutant mice. The PCR primers used and their relative locations within the CD3-ε gene are depicted with labeled arrows in the top diagram. Also indicated are the position of the ATG start codon and of the *neo* cassette insertion. The RNA-PCR products were gel-fractionated, blotted and hybridized with an oligonucleotide probe corresponding to a sequence located to the 5′ side of primer b (bottom panel). The sizes of the products as predicted from the sequences are 507 and 291 bp. The mouse CD3-ε genotypes are indicated at the top of the gel for each amplified RNA sample. (**C**) Western blotting of wild-type and homozygote mutant thymocytes. Post-nuclear supernatants from digitonin lysates were run under reducing conditions on a 15% SDS–polyacrylamide gel, transferred to nitrocellulose and analyzed for CD3-ε expression using a rabbit antiserum raised against a peptide corresponding to the C-terminal 10 amino acids of the CD3-ε polypeptide. Lanes CD3-$\varepsilon^{+/+}$ and CD3-$\varepsilon^{\Delta5/\Delta5}$ have each been loaded with 200 μg of total protein. The positions of two molecular weight standards are indicated (in kDa).

refer to subsequently as CD3-$\varepsilon^{\Delta5}$, was still capable of directing the synthesis of CD3-ε polypeptides, however in minute amounts and deprived of the extracellular domain encoded by exon 5.

The mouse CD3-γ, -δ and -ε genes reside within 50 kb of each other on chromosome 9 (Letourneur *et al.*, 1989). Owing to this linkage, it was important to demonstrate whether the introduction of a pgk–neo cassette into the CD3-ε transcription unit affected the expression of the neighboring CD3-γ and -δ genes. We found, by Northern blotting of total RNA extracted from wild-type, CD3-$\varepsilon^{\Delta5/\Delta5}$, RAG-$1^{-/-}$ and CD3-$\zeta/\eta^{-/-}$ thymuses, that the CD3-$\varepsilon^{\Delta5/\Delta5}$ mice displayed both a reduction in the amounts of CD3-γ transcripts and an absence of detectable CD3-δ transcripts (Figure 2). In contrast, the expression of the CD3-ζ gene which is unlinked to the CD3-γδε cluster was not markedly decreased in the CD3-$\varepsilon^{\Delta5/\Delta5}$ thymocytes. These results were somewhat unexpected, given that no alteration of the CD3-γδε gene cluster was detectable by Southern blot analysis other than the intended CD3-$\varepsilon^{\Delta5}$ mutation (data not shown). In support of the data suggesting that the integrity of the contiguous CD3-δ gene has been preserved during the targeting process, low levels of full-length CD3-δ transcripts were detected in CD3-$\varepsilon^{\Delta5/\Delta5}$ thymocytes using RNA-PCR (data not shown). Taken together, these data indicate that the insertion of a neomycin resistance cassette in place of exon 5 of the CD3-ε gene prevented the synthesis of intact CD3-ε polypeptides, and decreased the transcription of the neighboring CD3-δ and CD3-γ genes.

### *T cell populations in CD3-$\varepsilon^{\Delta5/\Delta5}$ mice*

When housed under specific pathogen-free conditions, CD3-$\varepsilon^{\Delta5/\Delta5}$ mice showed no differences in size, life span up to 1 year and reproductive ability relative to littermate controls. In sharp contrast to CD3-ζ/η-deficient mice, no overt sign of chronic intestinal inflammation (e.g. dilatation of the rectum and colon, enlargement of the mesenteric lymph nodes, diarrhea, etc.) was noticed in CD3- $\varepsilon^{\Delta5/\Delta5}$ mice. Moreover, non-lymphoid organs showed no evidence

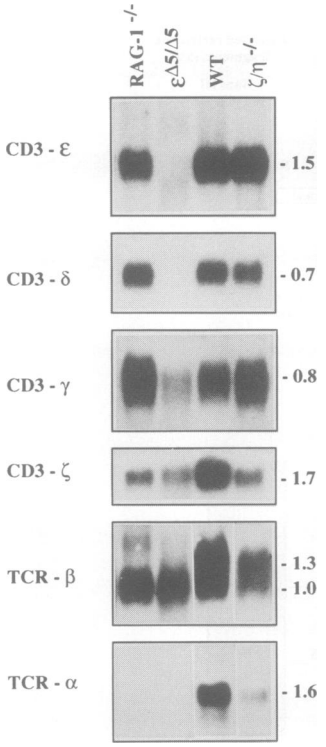


**Fig. 2.** Northern blot analysis of wild-type (WT), RAG-$1^{-/-}$, CD3-$\varepsilon^{\Delta5/\Delta5}$ and CD3-$\zeta/\eta^{-/-}$ thymocytes. Blots were hybridized with probes corresponding to CD3-ε, CD3-δ, CD3-γ, CD3-ζ, TCR-Cβ or TCR-Cα. To control the quantity and quality of RNA, each blot was subsequently stripped and re-analyzed with a 5′-kinased oligonucleotide specific for 28S rRNA (data not shown). The relative sizes of the bands are indicated in the right margin.

of gross morphological abnormalities. However, the thymus from CD3- $\varepsilon^{\Delta5/\Delta5}$ mice had dramatically reduced cell numbers (average $5.6\times10^6$) relative to littermate controls (average $220\times10^6$). In contrast to the situation previously reported for the CD3-ζ/η-deficient mice (Malissen *et al.*, 1993), no substantial interindividual variations were observed in the total numbers of thymocytes found in CD3-$\varepsilon^{\Delta5/\Delta5}$ mice. When analyzed by flow cytometry, CD3-$\varepsilon^{\Delta5/\Delta5}$ thymuses were found totally devoid of double- and single-positive cells, but retained almost normal absolute numbers of triple-negative cells (Figures 3 and 4). Moreover, almost all of the CD3-$\varepsilon^{\Delta5/\Delta5}$ thymocytes were Thy-$1^+$, $HSA^+$ and $CD5^{dull}$ (data not shown). Also shown in Figure 3 is a comparison of the CD3-$\varepsilon^{\Delta5/\Delta5}$ thymocytes with those found in mice carrying null mutation in the RAG-1 or CD3-ζ/η genes. Based on the expression of the CD4, CD8 and TCR molecules, the cell size and the total cell number counts, the CD3-$\varepsilon^{\Delta5}$ mutation appeared to arrest thymocyte differentiation at the very same developmental stage as a mutation in the RAG-1 gene (Figure 3). Furthermore, it is worth noticing that thymocyte differentiation was blocked by the CD3-$\varepsilon^{\Delta5}$ mutation at an earlier stage than by the CD3-ζ/η mutation.

To determine whether the CD3-$\varepsilon^{\Delta5}$ mutation prevented TCR expression at the surface of developing T cells, thymocytes from CD3-$\varepsilon^{+/+}$ and CD3-$\varepsilon^{\Delta5/\Delta5}$ mice were analyzed by two-color cytofluorometry using combinations of antibodies specific for the CD3-ε, TCR αβ or TCR γδ molecules. As shown in Figure 4 (upper panels), the CD3-$\varepsilon^{\Delta5}$ mutation resulted in the complete absence of T cells expressing low or high levels of TCR αβ heterodimers. In addition, staining with an anti-TCR δ antibody failed to detect any TCR $\gamma\delta^+$ T cells in CD3-$\varepsilon^{\Delta5/\Delta5}$ thymocytes (Figure 4, lower panels).

The lymph nodes and spleen of CD3-$\varepsilon^{\Delta5/\Delta5}$ mice did not contain any cells staining with antibodies specific for the CD3-ε, TCR αβ or TCR γδ molecules (data not shown). When analyzed for surface expression of CD4, CD8, Thy1 and B220, CD3-$\varepsilon^{\Delta5/\Delta5}$ lymph node cells were found to contain a few single-positive cells as well as residual Thy$1^+$ $B220^-$ cells (Figure 5). However, in contrast to the wild-type cell population, when analyzed by three-color cytofluorometry using various combinations of antibodies specific for the CD4, CD8, Thy 1 or B220 molecules, only a small fraction (<5%) of the Thy$1^+$$B220^-$ cells found in CD3- $\varepsilon^{\Delta5/\Delta5}$ lymph nodes expressed either the CD4 or CD8 molecules. Due to their small size, we have not been able to characterize these subsets further and determine their developmental origin. It is worth noting that normal numbers of B cells were present in lymph nodes of the mutant mice, as assessed by staining for B220 (Figure 5). No TCR–CD3 complexes were detected at the surface of the gut intraepithelial lymphocyte population (data not shown). Finally, T cell development proceeded normally in CD3-$\varepsilon^{\Delta5/+}$ heterozygous mice and the surface levels of TCR/CD3 complexes found on their thymocytes and mature T cells were identical to those of wild-type littermates (data not shown), arguing against a major dominant-negative effect exerted by the low levels of CD3-$\varepsilon^{\Delta5}$ polypeptides originating from the mutated CD3-ε allele.

### *Thymocyte subpopulations in CD3-$\varepsilon^{\Delta5/\Delta5}$ mice*

To specify the degree of coincidence existing between the developmental arrest points observed in the CD3-$\varepsilon^{\Delta5/\Delta5}$ and RAG-$1^{-/-}$ thymus, three-color flow cytometry was used to monitor the corresponding triple-negative T cell populations for the expression of CD25 and CD44 (Figure 6). Using this approach, four distinct triple-negative subsets can be identified in wild-type mice, and organized in the following developmental sequence $CD44^+CD25^- \rightarrow CD44^+CD25^+ \rightarrow CD44^{-/low}CD25^+ \rightarrow CD44^{-/low}CD25^-$ (Godfrey *et al.*, 1994). Two points should be made regarding this approach. First, because they express CD4 at levels low enough to be included in the electronic gate used to define the triple-negative T cells, the earliest $CD4^{low}CD8^-CD3^-$ precursors score as triple-negative cells and constitute part of the first subset of this sequence (Godfrey *et al.*, 1994). Second, the $CD44^{-/low}CD25^-$ cells which define the last subset of triple-negative cells, start to express CD3, CD4 and CD8 molecules at their surface but at levels not yet sufficient to allow them to be scored by flow cytometry as immature single positive or double-positive cells (Nikolic Zugic, 1991).

As shown in Figure 6, the triple-negative thymocytes found in both the RAG-$1^{-/-}$ and CD3-$\varepsilon^{\Delta5/\Delta5}$ mice were unable to progress beyond the $CD44^{-/low}CD25^+$ stage. Not only the $CD44^{-/low}CD25^-$ cells proper, but also most of the $CD44^{-/low}CD25^{low\ to\ -}$ intermediates linking them with the $CD44^{-/low}CD25^+$ subset were also missing in these two mutants. In contrast, the RAG-$1^{-/-}$ and CD3-$\varepsilon^{\Delta5/\Delta5}$ mutant mice showed no gross distortion in the absolute number of cells belonging to the triple-negative

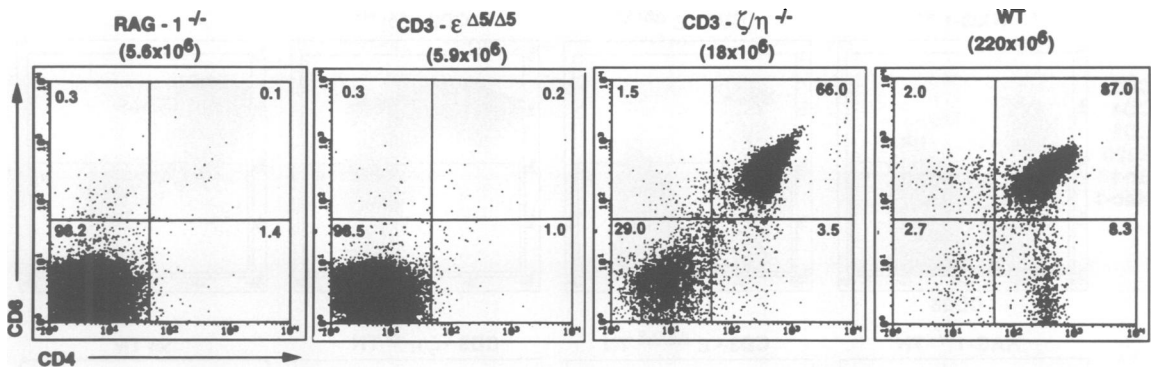


**Fig. 3.** The CD3-$\varepsilon^{\Delta 5/\Delta 5}$ mutation blocks thymocyte development at the $CD4^-CD8^-$ double-negative stage. Thymocytes from RAG-$1^{-/-}$, CD3-$\varepsilon^{\Delta 5/\Delta 5}$, CD3-$\zeta/\eta^{-/-}$ and wild-type (WT) mice were analyzed by flow cytometry for the expression of CD4 versus CD8. The percentage of cells found in each quadrant is indicated. The total averaged numbers of thymocytes found in each type of mouse are indicated above the corresponding dot displays.

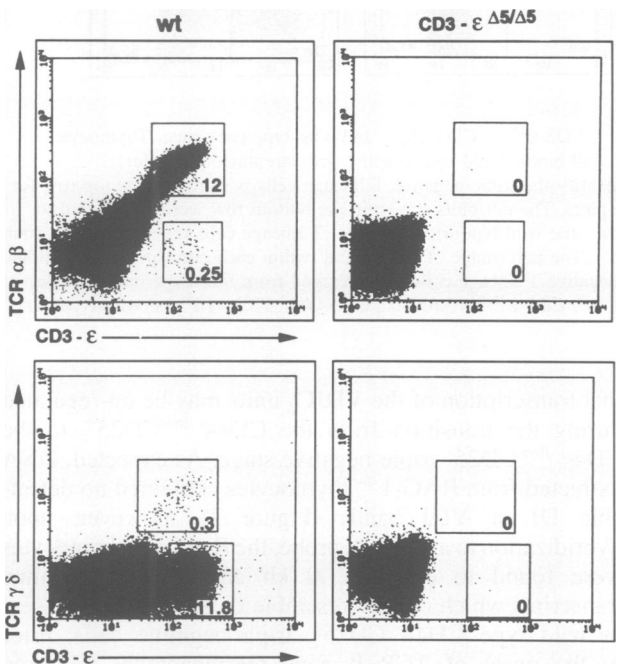


**Fig. 4.** Thymocytes from CD3-$\varepsilon^{\Delta 5/\Delta 5}$ mutant mice do not express detectable levels of TCR αβ or TCR γδ heterodimers at their cell surface. Thymocytes from a wild-type littermate (wt) or from a mouse homozygous for the CD3-ε mutation (CD3-$\varepsilon^{\Delta 5/\Delta 5}$) were analyzed by two-color flow cytometry for the expression of TCR αβ versus CD3-ε (top row) and TCR γδ versus CD3-ε (bottom row). Windows were set for each of the four panels on CD3-$\varepsilon^+$ TCR $\alpha\beta^{high}$ and CD3-$\varepsilon^+$ TCR $\gamma\delta^+$ subpopulations. The percentage of cells found in each window is indicated. $5\times10^5$ cells were analyzed per dot plot. It should be noted that the 2C11 anti-CD3-ε antibody used in this experiment is directed against the ectodomain of the CD3-ε chain. The exon coding for this domain has been deleted in the CD3-$\varepsilon^{\Delta 5}$ gene. Accordingly, the TCR-positive cells that may have developed in the CD3-$\varepsilon^{\Delta 5/\Delta 5}$ thymuses should have scored in the $TCR^+$ CD3-$\varepsilon^-$, upper left quadrant of each of the CD3-$\varepsilon^{\Delta 5/\Delta 5}$ dot plots.

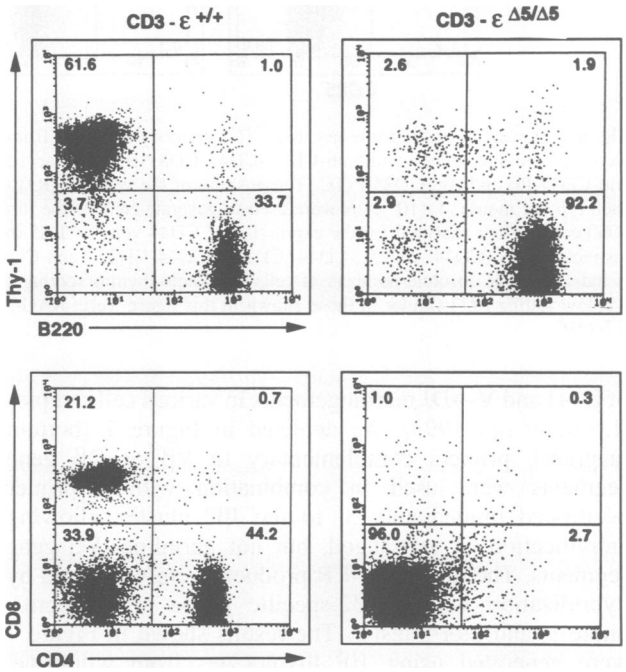


**Fig. 5.** Cytofluorometric analysis of peripheral T cells. Lymph node cells from CD3-$\varepsilon^{\Delta 5/\Delta 5}$ mice or control littermates (CD3-$\varepsilon^{+/+}$) were analyzed by two-color cytometry for the expression of Thy-1 versus B220 (top row), and CD4 versus CD8 (bottom row). The percentages of cells found in each quadrant are indicated.

cell subsets preceding the developmental arrest point (Figure 6). Therefore, on the basis of their cell surface phenotype, the triple-negative cells found in the CD3-$\varepsilon^{\Delta 5}$ and RAG-1 mutant mice appear arrested at the same developmental stage. As shown in Figure 3, T cell development in the CD3-ζ/η- deficient mice ends up at the double-positive stage. Accordingly, the triple-negative maturation sequence should not have been affected by the CD3-ζ/η mutation. However, consistent with previous results obtained using a different approach (Crompton *et al.*, 1994), the $CD44^{-/low}CD25^-$ cells, which constitute the immediate precursors of the double-positive cells, were almost absent from the thymus of CD3-$\zeta/\eta^{-/-}$ mice (Figure 6).

### *TCR β gene rearrangements and transcription in CD3-$\varepsilon^{\Delta 5/\Delta 5}$ mice*

The thymocytes found in CD3-$\varepsilon^{\Delta 5/\Delta 5}$ mutant mice are capable of reaching the $CD44^{-/low}CD25^+$ triple-negative phenotypic stage during which TCR β gene rearrangement normally happens. To determine the impact of the CD3-$\varepsilon^{\Delta 5}$ mutation on the occurrence of TCR β rearrangement, we analyzed the status of the TCR β loci using a DNA-PCR assay, which provides an estimation of the relative levels

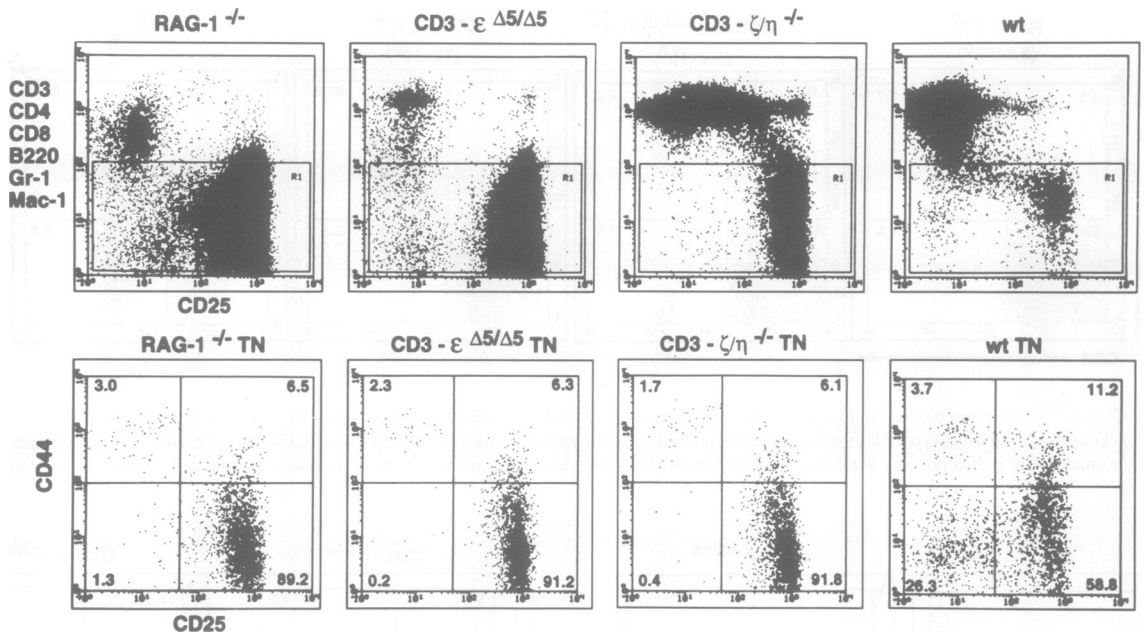


**Fig. 6.** Comparison of the triple-negative (TN) thymocyte subsets from RAG-1$^{-/-}$, CD3-ε$^{\Delta5/\Delta5}$, CD3-ζ/η$^{-/-}$ and wild-type (wt) mice. Thymocytes were isolated and stained with anti-CD3, -CD4, -CD8, -B220, -Mac-1 and -Gr-1 (all biotinylated and detected with streptavidin-tricolor), anti-CD44-PE and anti-CD25-FITC. The position of the window (R1) used to identify the triple-negative T lineage cells is shown in the top row for each type of mouse. $5\times10^5$ cells were used to generate each of the top row dot plots. The dot plots shown in the bottom row were normalized to 2000 cells. When analyzed for the expression of CD44 versus CD25 (bottom row), the wild-type triple-negative T lineage cells revealed at least four distinct subsets (CD44$^+$CD25$^-$, CD44$^+$CD25$^+$, CD44$^-$CD25$^+$ and CD44$^-$CD25$^-$). The percentage of cells found within each corresponding quadrant is indicated. The absolute numbers of cells per whole thymus scoring as triple-negative T lineage cells and averaged from four experiments using window setting (R1) similar to those shown in this figure were: RAG-1$^{-/-}$: $5.3\times10^6$, CD3-ε$^{\Delta5/\Delta5}$: $5.6\times10^6$, CD3-ζ/η$^{-/-}$: $3.1\times10^6$ and wild-type: $6.7\times10^6$.

of D→J and V→DJ rearrangements in various cell samples (Levin *et al.*, 1993). As depicted in Figure 7 (bottom diagram), primers complementary to Vβ or Dβ gene segments were used in combination with a primer positioned immediately 3′ to the Jβ2 cluster, allowing amplification of rearranged, but not germline, Vβ gene segments. The resulting PCR products were visualized by hybridization with a Jβ2-specific probe after electrophoresis and blot transfer. The results shown in Figure 7 were generated using $10^5$ thymocytes from wild-type, RAG-1$^{-/-}$, CD3-ε$^{\Delta5/\Delta5}$ or CD3-ζ/η$^{-/-}$ mice and corresponded to rearrangements of Dβ2 (top), Vβ8 (middle) and Vβ11 (bottom) to each of the six Jβ2 gene segments. As indicated by the disappearance of germline band (GL) and the presence of several bands corresponding to DJ rearrangements, CD3-ε$^{\Delta5/\Delta5}$ thymocytes contained D→J rearrangements which were almost as extensive as those found in wild-type and CD3-ζ/η$^{-/-}$ mice. Moreover, the levels of 1.0 kb DJC$_\beta$ transcripts detected in Northern blot of CD3-ε$^{\Delta5/\Delta5}$ thymocytes corroborated these rearrangement results (Figure 2). V→DJ rearrangements were also readily detectable in the thymuses of CD3-ε$^{\Delta5/\Delta5}$ (as well as CD3-ζ/η) mutant mice (Figure 7). However, a sensitive RNA-PCR assay was needed to ascertain unambiguously the presence of 1.3 kb VDJC$_\beta$ transcripts in the CD3-ε$^{\Delta5/\Delta5}$ thymocytes (compare Figures 3 and 8). Therefore, when compared with wild-type and CD3-ζ/η$^{-/-}$ mice, the thymocytes found in CD3-ε$^{\Delta5/\Delta5}$ mice showed a lack of correlation between the extent of VDJ rearrangements (Figure 7) and levels of VDJC$_\beta$ transcription (Figure 8). Considering that the CD3-ε$^{\Delta5/\Delta5}$ thymus includes mostly CD44$^{-/low}$CD25$^+$ cells (Figure 6), these results suggest that transcription of the VDJC$_\beta$ units may be up-regulated during the transition from the CD44$^{-/low}$CD25$^+$ to the CD44$^{-/low}$CD25$^-$ triple-negative stage. As expected, DNA extracted from RAG-1$^{-/-}$ thymocytes contained no detectable DJ or VDJ bands (Figure 7). However, upon hybridization to a TCR Cβ probe, the RAG-1$^{-/-}$ thymocytes were found to express 1.0 kb and 1.6 kb germline transcripts which closely resemble those normally present in wild type CD44$^+$CD25$^+$ triple-negative cells, prior to the onset of TCR β gene rearrangement (Godfrey *et al.*, 1994).

### *TCR α gene rearrangement in CD3-ε$^{\Delta5/\Delta5}$ mice*

The TCR α chain locus consists of ~100 V gene segments which map 5′ to a cluster of 49 Jα gene segments spread over 60 kb of DNA (reviewed in Malissen *et al.*, 1992). Such an extended chromosomal organization has hampered the analysis of TCR α rearrangement during thymic differentiation. Accordingly, most of the data regarding this locus have been inferred indirectly from the analysis of TCR α mRNA expression. The CD3-ε$^{\Delta5/\Delta5}$ mice constitute an enriched source of RAG-positive, CD44$^{-/low}$CD25$^+$ thymocytes which are devoid of contaminating downstream subsets (Figure 6) and may serve to determine whether TCR α rearrangement can occur at the CD44$^{-/low}$CD25$^+$ stage concurrently with TCR β rearrangement. Using a DNA-PCR assay which detects the rearrangement of the Vα2 or Vα8 subfamily members to the Jα25 gene segment, we found no VJ band in the CD3-ε$^{\Delta5/\Delta5}$ and CD3-ζ/η$^{-/-}$ thymocytes (data not shown). However, although somewhat reduced when compared with wild-type, Vα2- and Vα8-containing transcripts of

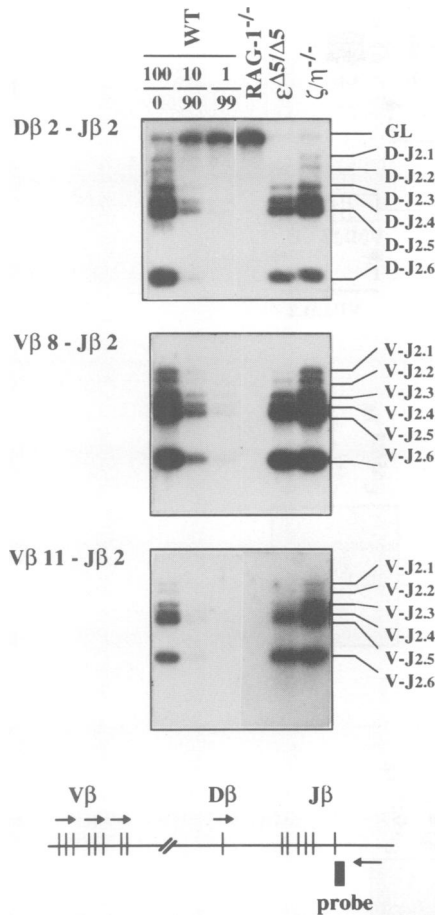


**Fig. 7.** Relative levels of TCRβ gene rearrangements in RAG-$1^{-/-}$, CD3-$\varepsilon^{\Delta5/\Delta5}$, CD3-$\zeta/\eta^{-/-}$ and wild-type (wt) thymocytes. The extent of Dβ–Jβ and Vβ–DβJβ rearrangements were analyzed by DNA-PCR. The relative positions of the PCR primers within the TCR β locus are depicted in the bottom diagram. Products derived from PCR reactions involving the Jβ2 3′ primer with Dβ2- (top), Vβ8- (middle) or Vβ11- (bottom) specific 5′ primers were gel-fractionated and hybridized with the Jβ2-specific probe depicted at the bottom (probe). Sources of thymocyte DNA are indicated above each lane. The positions of the products corresponding to the germline (DβJβ) cluster (GL) and specific Dβ–Jβ and Vβ–DβJβ rearrangements are indicated in the right margin. Serial 10-fold dilutions have been analyzed for wild-type thymic DNA. For each dilution, template DNA was kept constant by adding ES cell DNA that carries no TCR rearrangement in the proportion indicated above each lane (100 corresponding to $10^5$ cells).

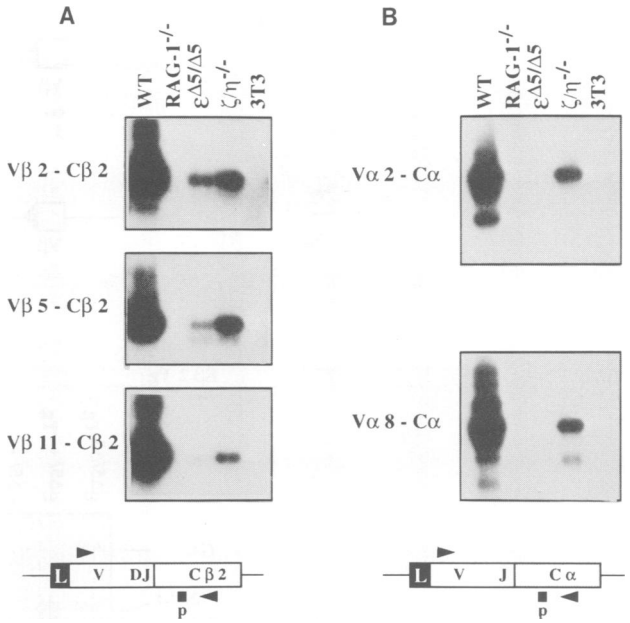


**Fig. 8.** Transcription of the TCR α and TCR β loci in RAG-$1^{-/-}$, CD3-$\varepsilon^{\Delta5/\Delta5}$, CD3-$\zeta/\eta^{-/-}$ and wild-type (wt) thymocytes. The presence of transcripts originating from rearranged TCR α and TCR β genes was assessed by RNA-PCR using the strategy depicted in the bottom diagrams. (**A**) TCR β transcripts. A Cβ2 antisense primer was used in combination with a sense primer specific for the Vβ2 (top), Vβ5 (middle) or Vβ11 (bottom) gene segments. The RNA-PCR products were gel-fractionated, blotted and hybridized with a Cβ2-specific probe (denoted as p in the bottom diagram). (**B**) TCR α transcripts. A Cα antisense primer was used in combination with primers specific for all the members of the Vα2 (top) or Vα8 (bottom) subfamilies. The RNA-PCR products were hybridized with a Cα-specific probe (denoted as p in the bottom diagram). RNA-PCR reactions using a pair of primers specific for the actin gene were set up in parallel to control for the quality and quantity of cDNA template in each sample (data not shown). RNA extracted from negative control NIH 3T3 fibroblastic cells was also included. The autoradiographs have been purposely overexposed to underscore the absence of TCR α transcripts in the CD3-$\varepsilon^{\Delta5/\Delta5}$ samples.

sizes expected for rearranged V genes were clearly present in the CD3-$\zeta/\eta^{-/-}$ thymocytes (Figures 2 and 8). Therefore, the inability to detect the corresponding VJ bands in the CD3-$\zeta/\eta^{-/-}$ thymic DNA samples indicated that our DNA-PCR assay is not sensitive enough to analyze the status of the TCR α locus in the CD3-deficient mice, inasmuch as it samples only a few (<10) of the ~4900 V×J combinations theoretically permitted at the TCR α locus. Moreover, despite the greater sensitivity of our RNA-PCR assay, the absence of detectable TCR α transcripts in the CD3-$\varepsilon^{\Delta5/\Delta5}$ thymocytes did not exclude the fact that they may still contain low levels of poorly transcribed TCR α genes. To alleviate part of the sensitivity problem and determine whether the $CD44^{-/low}CD25^{+}$ cells found in the CD3-$\varepsilon^{\Delta5/\Delta5}$ mice can perform TCR α rearrangement, transgenic mice carrying artificial VDJ recombination substrates associated with either the TCR β (Eβ) or TCRα (Eα) gene enhancers were crossed with CD3-$\varepsilon^{\Delta5/\Delta5}$ mice. When introduced into wild-type mice, these Eβ- and Eα-containing substrates showed patterns of DJ and VDJ rearrangements with lineage and cell stage specificities remarkably similar to those of endogeneous TCR β and TCR α loci, respectively (Capone *et al.*, 1993). In contrast to endogeneous TCR loci, both reporter substrates allow very limited numbers of DJ and VDJ combinations, the relative levels of which can be determined using a DNA-PCR assay (Capone *et al.*, 1993). Figure 9 shows results from analysis of thymocytes from Eβ transgenic (Eβ2 Tg, panel B) and Eα transgenic (Eα1 Tg, panel C) CD3-$\varepsilon^{\Delta5/\Delta5}$ mice. Fragments corresponding to substrate DβJβ and VβDβJβ rearrangements were detectable in Eβ2 transgenic CD3-$\varepsilon^{\Delta5/\Delta5}$ mice, although their extent was lower than in the Eβ2 transgenic CD3-$\varepsilon^{\Delta5/+}$ control littermates. However, no difference in the extent of substrate rearrangement was found when the Eβ2 transgenic CD3-$\varepsilon^{\Delta5/\Delta5}$ thymocytes, consisting of >90% $CD25^{+}$ triple-negative cells, were more appropriately compared with $CD25^{+}$ triple-negative cells sorted from wild-type thymus (compare Figure 9B with Figures 6 and 7 in Capone *et al.*, 1993). Therefore, these results corroborated the observation that CD3-$\varepsilon^{\Delta5/\Delta5}$ thymocytes do assemble their

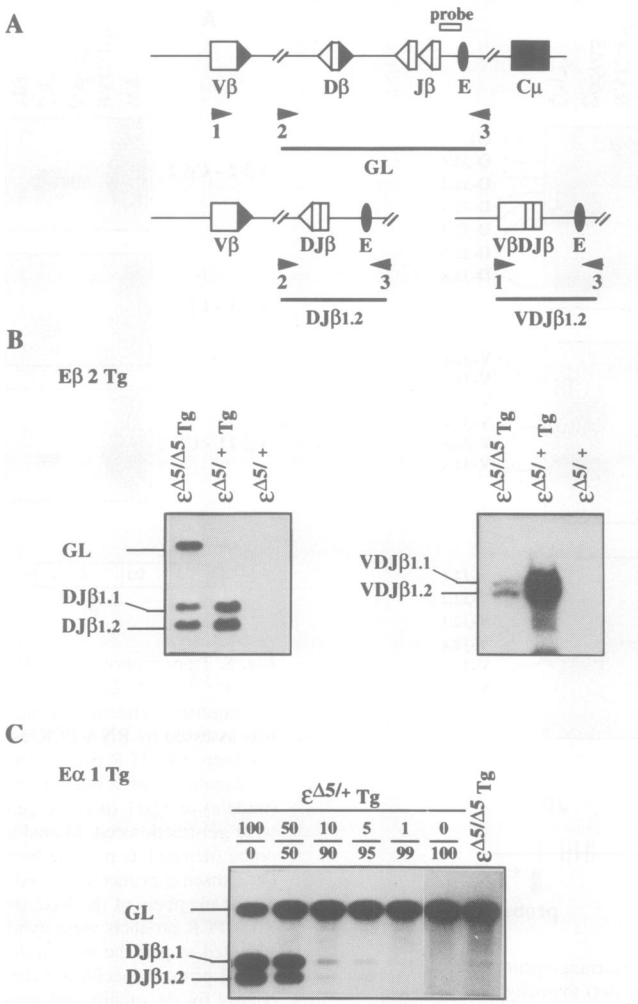


**Fig. 9.** Rearrangements of VDJ recombination substrates in thymocytes from crosses between CD3-$\varepsilon^{\Delta5/\Delta5}$ mutant mice and transgenic mice containing a VDJ recombination substrate controlled by either the TCR β (Eβ2 Tg) or TCR α (Eα1 Tg) enhancer. Both reporter substrates comprise germline Vβ, Dβ and Jβ gene segments linked to an IgH region containing the Cμ gene. In addition to these shared elements, they include either the TCR β or TCR α locus enhancer (Capone *et al.*, 1993). (**A**) Schematic diagram of the DNA-PCR assay used to assess the rearrangement status of the recombination substrates. The position and designation of the primers used in the assay are indicated below diagrams of unrearranged (top) and rearranged (bottom) recombination substrates. The V, D and J gene segments are indicated by open boxes, their flanking recombination signal sequences by triangles, the TCR enhancer by a shaded ellipsoid and the Cμ exons by a shaded box. Three of the five predicted PCR products are shown as shaded bars. They correspond to the unrearranged DJ cluster (GL) and to DJ or VDJ rearrangements involving Jβ1.2 (the two products involving Jβ1.1 are not shown). Note that, in germline configuration, the unrearranged fragment located between primers 1 and 3 is too large to be amplified by PCR. (**B**) TCR Eβ recombination substrate. Products derived from PCR reactions performed on a DNA template equivalent to $5\times10^3$ cells and using primer pairs 2 + 3 (left panel) or 1 + 3 (right panel) were gel-fractionated and hybridized to a probe internal to the amplified fragments (denoted as probe in A). Sources of thymocyte DNA are indicated above each lane. The positions of the bands corresponding to the germline (GL) and rearranged products are indicated in the margins. The presence of two rearranged bands is accounted for by the fact that the Dβ1 gene segment can rearrange with either the Jβ1.1 or Jβ1.2 gene segments. (**C**) TCR Eα recombination substrate. Products derived from PCR reactions performed on a DNA template equivalent to $5\times10^3$ cells using primer pair 2 + 3 were processed as described for the TCR Eβ substrate. The level of sensitivity of the PCR assay was determined using serial dilutions of genomic DNA extracted from (CD3-$\varepsilon^{\Delta5/+}\times$Eα1Tg) thymocytes. For each dilution, input template DNA was kept constant by adding unrearranged kidney DNA extracted from (CD3- $\varepsilon^{\Delta5/+}\times$Eα1Tg) mice, in the proportion indicated above each lane (100 corresponding to $5\times10^3$ cells). Note that the extent of residual germline band detected in the substrate present in the Eα1 transgenic CD3- $\varepsilon^{\Delta5/+}$ mice suggested that it has a lower competence to rearrange relative to the substrate present in the Eβ2 transgenic line (compare lanes CD3- $\varepsilon^{\Delta5/+}$ Tg in B and C). As previously hypothesized, this decreased competence is probably due to the integration site or number of active transgene copies (Capone *et al.*, 1993).

endogenous TCR β genes (see above). In sharp contrast, substrate DβJβ rearrangements were dramatically reduced within the thymocytes from Eα1 transgenic CD3-$\varepsilon^{\Delta5/\Delta5}$ mice (Figure 9) and represented <5% that observed in Eα1 transgenic CD3-$\varepsilon^{\Delta5/+}$ control thymocytes. Therefore, in the CD3-$\varepsilon^{\Delta5/\Delta5}$ thymocytes, substrate recombinations controlled by the TCR α gene enhancer occurred far less readily than those activated by the TCR β gene enhancer.

### *Rearrangement of TCR γ and δ genes in CD3-$\varepsilon^{\Delta5/\Delta5}$ mice*

We next examined the effects of the CD3-$\varepsilon^{\Delta5}$ mutation on the rearrangement of TCR γ and δ genes using a DNA-PCR approach (Itohara *et al.*, 1993). As shown in Figure 10, the CD3-$\varepsilon^{\Delta5}$ mutation did not inhibit the rearrangement of TCR γ or TCR δ genes. Moreover, in both wild-type and CD3-$\varepsilon^{\Delta5/\Delta5}$ mutant mice, distinct pairs of gene

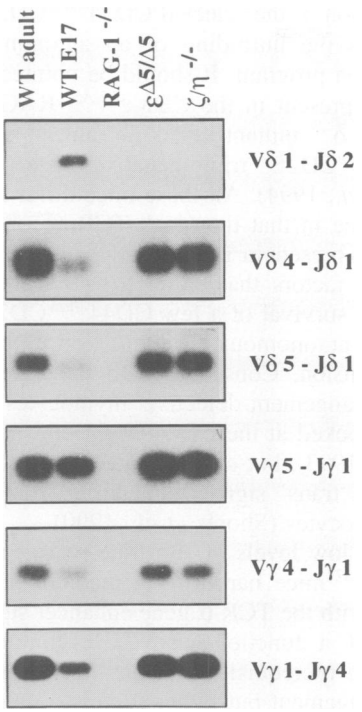


**Fig. 10.** Relative levels of TCR γ and TCR δ gene rearrangements in RAG-1$^{-/-}$, CD3-ε$^{\Delta5/\Delta5}$, CD3-ζ/η$^{-/-}$ and wild-type (wt) thymocytes. DNA extracted from thymocytes of fetuses at day 17 of gestation (wt E17) and of 4- to 6-week-old adult wild-type (wt adult) and mutant mice was amplified with PCR primer pairs specific for the Vδ1–Jδ2, Vδ4–Jδ1, Vδ5–Jδ1, Vγ5–Jγ1, Vγ4–Jγ1 and Vγ1–Jγ4 rearrangements. PCR products were gel-fractionated and the corresponding Southern blots were hybridized with labeled oligonucleotide probes.

segments were preferentially rearranged in fetal (day 17 of gestation) and adult (6-week-old) mice. For instance, the Vδ1–Jδ2 genes, which are generated only during the early fetal stages of thymic development, were absent in the adult thymus in both the CD3-ε$^{\Delta5}$ mutant and wild-type mice. Conversely, the usage of other Vγ and Vδ gene segments, especially Vγ1, Vγ4, Vδ4 and Vδ5, was predominant in the adult thymus in both the CD3-ε$^{\Delta5}$ mutant and wild-type mice. Therefore, the CD3-ε$^{\Delta5}$ (as well as CD3-ζ/η) mutation had little effect on both the extent and timing of TCR γ and δ gene rearrangements.

## Discussion

The CD3-ε gene has been targeted by replacing most of its exon 5 with a neomycin resistance cassette. This resulted in an internally expanded exon 5, bounded by normal splicing sites. As shown by RNA-PCR analysis, the altered exon was skipped during splicing events, an observation consistent with splicing models postulating pairing between the splice sites across an exon (Berget, 1995). Skipping of exon 5 resulted in the synthesis of limited amounts of CD3-ε polypeptides deprived of extracellular domain. In transfected COS cells, the CD3-ε ectodomain has been found mandatory for the proper assembly of CD3-ε with the CD3-γ, CD3-δ and TCR β polypeptides (Wileman *et al.*, 1993; Manolios *et al.*, 1994). Accordingly, if similar rules of TCR assembly apply to thymocytes, the few CD3-ε$^{\Delta5}$ polypeptides found in homozygous mutant mice should have lost their ability to participate in the formation of both γε and δε subcomplexes capable of interacting with TCR chains. Owing to both the small size of the CD3-ε$^{\Delta5/\Delta5}$ thymus and lack of transformed CD3-ε$^{\Delta5/\Delta5}$ pre-T cell lines, we have not been able to determine yet the direct effect of the CD3-ε$^{\Delta5}$ mutation on the assembly of the pre-TCR isoform. In the process of characterizing the CD3-ε$^{\Delta5/\Delta5}$ mice, we unexpectedly found that the presence of the *neo* cassette affected the expression of the neighboring CD3-δ and -γ genes. Gene targeting experiments aiming at the identification of *cis*-control elements involved in Ig gene rearrangements have already shown that the insertion of a *neo* cassette next to an enhancer sequence can distort the frequency of rearrangements of the targeted allele (Takeda *et al.*, 1993). As previously hypothesized for targeted Ig loci, there are several mechanisms by which the insertion of the *neo* cassette can possibly affect the transcription of the CD3-δ and -γ genes. One is disruption of an unknown element that is present within exon 5 and important for the regulation of the CD3-γδε cluster. Also, the coding sequence of the *neo* gene has been reported to have a suppressive effect on transcription (Artelt *et al.*, 1991). Therefore, its presence within the CD3-ε gene may act negatively on the transcription of the neighboring CD3-γ and -δ genes, as well as account for the presence of low steady-state levels of CD3-ε$^{\Delta5}$ transcripts. Discriminating between the above hypotheses will require the utilization of a *neo* cassette flanked by *lox P* sites and its subsequent removal from the ES cell genome by transient expression of the Cre recombinase (Gu *et al.*, 1993).

We demonstrated that the CD3-ε$^{\Delta5}$ mutation abolishes the expression of intact CD3-ε polypeptides and reduces the transcription rate of the CD3-γδε gene cluster. These cumulative effects should prevent the assembly of CD3-γε and -δε heterodimers and, thus, account for the fact that the CD3-ε$^{\Delta5/\Delta5}$ thymocytes do not progress beyond the CD44$^{-/low}$CD25$^{+}$ triple-negative stage. At that developmental stage, CD3-ε is likely to exert its effect as part of a pre-TCR complex involving the CD3-γ, CD3-ζ, pTα and TCR β polypeptides (Saint Ruf *et al.*, 1994). The thymocytes found in the CD3-ε$^{\Delta5/\Delta5}$ mice contain readily detectable levels of CD3-ζ, TCR β and pTα transcripts (data not shown and Figures 2 and 8). However, the lack of CD3-γε and -δε cores presumably prevents the pTα–TCR β and CD3-$\zeta_2$ dimers from participating in the assembly of a functional checkpoint apparatus. This would explain the fact that the CD3-ε$^{\Delta5}$ mutation has no discernible effect on the absolute number of CD44$^{-/low}$CD25$^{+}$ cells, and starts to become manifest first at the CD44$^{-/low}$CD25$^{+ \text{ to } -}$ transitional stage (Figure 6). In marked contrast, the CD44$^{-/low}$CD25$^{+}$ → CD44$^{-/low}$CD25$^{-}$ checkpoint can be activated, albeit inefficiently, in thymocytes deprived of CD3-ζ/η polypeptide (Liu *et al.*, 1993; Love *et al.*, 1993; Malissen *et al.*, 1993; Crompton *et al.*, 1994). The mandatory contribution of the CD3-ε-containing module (Wegener *et al.*, 1992) to the operation of this checkpoint is probably related to the nucleating role played by CD3-ε polypeptides in the assembly of the pre-TCR complex. Conversely, the CD3-ζ/η homodimers would merely constitute a dispensable amplification module for the pre-TCR complex, increasing its assembly rate and stability as well as contributing, via redundant signaling

motifs (Shinkai *et al.*, 1995), to the strengthening of its inductive signals.

Overexpression of various CD3-ε transgenes blocks thymocyte development at the $CD44^+CD25^-$ triple-negative stage and prevents natural killer (NK) cell development (Wang *et al.*, 1995). In contrast, CD3-$\varepsilon^{\Delta5/\Delta5}$ mutant mice have normal numbers of functional NK cells (Renard *et al.*, 1995), and produce T cells which can faithfully reach the $CD44^{-/low}CD25^+$ stage (Figure 6), suggesting that it is after that stage that the presence of intact CD3-ε protein is required. The discrepancy between these two phenotypes may be explained as follows. The CD3-ε polypeptides may be part of a putative pro-TCR complex expressed prior to the appearance of TCR β polypeptides (Wang *et al.*, 1994; Wiest *et al.*, 1994), and the function of which is abrogated by overexpressing CD3-ε protein, but complemented by the few truncated polypeptides found in the CD3-$\varepsilon^{\Delta5/\Delta5}$ mutant mice. Alternatively, when overexpressed, the CD3-ε polypeptides may sequester effector or adaptor molecules belonging to other signaling pathways involved in the progression to the $CD44^{-/low}CD25^+$ triple-negative stage.

TCR β gene rearrangements do occur in CD3-$\varepsilon^{\Delta5/\Delta5}$ thymocytes. However, in line with a previous analysis performed on $CD25^+$ triple-negative cells sorted from wild-type thymus (Dudley *et al.*, 1994; Godfrey *et al.*, 1994; Wilson and MacDonald, 1995), the CD3-$\varepsilon^{\Delta5/\Delta5}$ thymocytes contain low levels of full-length 1.3 kb TCR β transcripts, providing a potential for the synthesis of only minute amounts of TCR β polypeptides. Consistent with these observations, neither TCR β, nor CD3-ε polypeptides can be detected at the surface of wild-type thymocytes prior to the $CD44^{-/low}CD25^-$ stage (Wilson and MacDonald, 1995). It is worth noticing that in wild-type thymus, the few (< 10%) $CD25^+$ triple-negative cells expressing intracellular TCR β polypeptides display intermediate levels of CD25 and correspond probably to cells in transit to the $CD44^{-/low}CD25^-$ stage (Levelt *et al.*, 1993a). Therefore, the $CD44^{-/low}CD25^+$ population probably corresponds to a continuum of cells in the process of TCR β rearrangement, a majority of which still have not achieved the assembly of a pre-TCR complex.

The pre-TCR complex is likely to constitute a molecular sensor capable of monitoring productive TCR β gene rearrangements. According to that model, mice deficient in TCR β polypeptide should have resembled CD3-$\varepsilon^{\Delta5/\Delta5}$ mice and ranked as 'non-leaky' checkpoint mutants. However, the presence of small numbers of both $CD44^{-/low}CD25^-$ triple-negative and double-positive cells in TCR $\beta^{-/-}$ mutant mice (Mombaerts *et al.*, 1992; Godfrey *et al.*, 1994) contradicts the view that the activation of the $CD44^{-/low}CD25^+ \rightarrow CD44^{-/low}CD25^-$ checkpoint is totally coupled to the production of TCR β polypeptide, and further suggests that pre-TCR-independent pathway(s) can promote, albeit inefficiently, the transition through the $CD44^{-/low}CD25^+ \rightarrow CD44^{-/low}CD25^-$ checkpoint (Saint-Ruf *et al.*, 1994). For instance, as previously hypothesized for hematopoietic growth factor receptors (Fairbairn *et al.*, 1993) and the pre-B cell receptor (pre-BCR, Rolink *et al.*, 1994), the primary role of the pre-TCR may be enabling rather than inductive. Accordingly, the checkpoint operated by the pre-TCR may not be needed for differentiation to occur but rather triggers signals that promote the survival and/or proliferation of the selected $CD44^{-/low}CD25^+$ cells and thus permits the unfolding of an autonomous internal differentiation program. It should be pointed out that the thymocytes present in the CD3-$\varepsilon^{\Delta5/\Delta5}$, $RAG^{-/-}$ and TCR $\beta^{-/-} \times$TCR $\delta^{-/-}$ mutant mice do not progress beyond the $CD44^{-/low}CD25^+$ triple-negative stage (Figure 6 and Godfrey *et al.*, 1994). All these mice differ from TCR β-deficient mice in that they lack TCR $\gamma\delta^+$ T cells. Thus, the γδ T cells present in TCR $\beta^{-/-}$ mice may possibly release intercellular factors that either trigger differentiation or promote the survival of a few $CD44^{-/low}CD25^+$ cells and permit their autonomous differentiation in the absence of clonal expansion. Consistent with the latter possibility, V(D)J rearrangement-defective thymocytes from SCID mice are blocked at the $CD44^{-/low}CD25^+$ stage (Rothenberg *et al.*, 1993), but can be induced to become double-positive by 'trans' signals emanating from neighboring $TCR^+$ thymocytes (Shores *et al.*, 1990).

The very low levels of substrate rearrangement found in CD3-$\varepsilon^{\Delta5/\Delta5}$ mice harboring a recombination substrate associated with the TCR α gene enhancer suggest that the assembly of a functional pre-TCR complex does not constitute a prerequisite for the initiation of TCR α gene rearrangement but rather serves to up-regulate their frequency. Whether these low levels of substrate rearrangement genuinely mimic the situation at the endogeneous TCR α locus will await the development of a more sensitive PCR-based analysis of α chain gene rearrangement. However, a definitive test for the occurrence of TCR α chain gene rearrangement prior to the transition to the $CD44^{-/low}CD25^-$ stage will probably emerge from the analysis of pTα-deficient mice. For instance, if TCR α chain gene rearrangements occur with low incidence in the $CD44^{-/low}CD25^+$ subset, the rare cells capable of productively rearranging both their TCR α and β loci will assemble a TCR αβ/CD3 complex, thereby bypassing the requirement for a pre-TCR complex. In $pT\alpha^{-/-}$ mice, these rare triple-negative cells will differentiate (see Takahama *et al.*, 1992) and slowly fill the pool of mature T cells, in a mode analogous to the B cells present in mice deficient in the λ5 subunit of the pre-BCR (Ehlich *et al.*, 1993). According to this hypothesis, the $pT\alpha^{-/-}$ mice will be capable of producing mature T cells and thus will differ dramatically from the CD3-$\varepsilon^{\Delta5/\Delta5}$ mice. Conversely, in the absence of TCR α gene rearrangement in the $CD44^{-/low}CD25^+$ subset, the thymocytes present in $pT\alpha^{-/-}$ mice are likely to be arrested at the very same developmental stage as those present in the CD3-$\varepsilon^{\Delta5/\Delta5}$ mice.

Finally, our data also bear on the mechanisms controlling the differentiation of γδ T cells. If γδ T cell development proceeds similarly to αβ T cell developement, a pre-Tδ (pTδ) chain is likely to exist and contribute to the formation of a TCR γ–pTδ/CD3 complex, the function of which may consist in up-regulating TCR δ rearrangement subsequent to the achievement of productive TCR γ rearrangement. However, we found that the CD3-$\varepsilon^{\Delta5}$ mutation has no discernible effect on the completion of TCR γ and TCR δ rearrangements. Therefore, the latter may not be subjected to epigenetic controls similar to those operating on the expression of TCR α and β genes (see also Itohara *et al.*, 1993). Conversely, the CD3 components required for the operation of this putative TCR γ–pTδ receptor

may be distinct from those used by the TCR β–pTα complex.

## Materials and methods

### Vector construction

A mouse CD3-ε genomic clone was isolated from a B10.A genomic phage library. A 6.5 kb *Hin*dIII restriction fragment containing exons 5–8 was isolated from this genomic clone and blunt-end ligated into plasmid pBS-SKII (Stratagene). A 168 bp *Xba*I–*Xho*I fragment encompassing most of exon 5 was deleted and replaced by a 1.8 kb pgk–neo cassette (*neo*) derived from plasmid pKJ.1 (Mc Burney *et al.*, 1991). Finally, a 1.9 kb herpes simplex thymidine kinase (TK) cassette derived from plasmid pMC1-tk (Mansour *et al.*, 1988) was cloned in the *Not*I site present in the polylinker located at the 3′ end of the CD3-ε insert. The resulting targeting construct is denoted pRH20A and depicted in Figure 1A.

### Transfection and screening of CD3-ε mutant cell clones

The Bruce 4 ES cell line derives from C57BL/6 mice and was transfected as previously described (Malissen *et al.*, 1993). After selection in the presence of G418 and gancyclovir, colonies were harvested and transferred into 96-well plates. After 3 days, the plates were duplicated. Colonies from one set of plates were screened for homologous recombinants by Southern blot analysis using the probe depicted in Figure 1A. Finally, a *neo* probe was used to ensure that adventitious non-homologous recombinants had not occurred in the selected clones.

### Production of CD3-$\varepsilon^{\Delta 5/\Delta 5}$ mice

Chimeras were generated essentially as described by Bradley (1987). Briefly, ~10 mutant ES cells were injected into BALB/c blastocysts collected at 3.5 days post-coitus. Injected blastocysts were re-implanted into the uteri of pseudopregrant C57BL/6×CBA/J F1 females. Chimeric progeny were identified by coat color and chimeric males mated to C57BL/6 females. CD3-$\varepsilon^{\Delta 5/+}$ heterozygous mice were intercrossed to produce homozygous CD3-$\varepsilon^{\Delta 5/\Delta 5}$ mice. Screening of mice for the CD3-ε mutation was performed by Southern blot analysis.

### Mice

Mice maintained under specific pathogen-free (SPF) conditions were between 2 weeks and 2 months old when analyzed. RAG-$1^{-/-}$-deficient mice were originally obtained from E.Spanopoulou (Spanopoulou *et al.*, 1994). The CD3-ζ/η-deficient line has been described (Malissen *et al.*, 1993). Transgenic mice carrying a VDJ recombination substrate under the control of the TCR α (line Eα 1) or TCRβ (line Eβ2) enhancer have been described previously (Capone *et al.*, 1993). These transgenic mice were crossed with CD3-$\varepsilon^{\Delta 5}$ mice. Mice expressing the Eα1 or Eβ2 transgene were then backrossed to CD3-$\varepsilon^{\Delta 5}$ mice to obtain homozygous CD3-$\varepsilon^{\Delta 5/\Delta 5}$ mutants expressing an Eβ2 or Eα1 transgene.

### Northern blot analysis

Northern blot analysis was performed on total RNA as previously described (Malissen *et al.*, 1988). Hybridization probes corresponding to the TCR Cα and TCR Cβ regions and to each of the CD3 subunits were derived as previously described (Letourneur and Malissen, 1989; Wegener *et al.*, 1992). Controls for the quality and quantity of RNA prepared from the various thymocyte populations were performed using a 5′-kinased oligonucleotide specific for the 28S rRNA (5′ TGAATCC-TCCGGGCGGACT 3′).

### Western blot analysis

Thymocytes from wild-type and mutant mice were solubilized in digitonin lysis buffer (1% digitonin, 0.1% Triton X-100, 150 mM NaCl, 1 mM EDTA, 1 mM phenylmethylsulfonyl fluoride, 10 μg/ml aprotinin, 10 μg/ml leupeptine, 10 mM triethanolamine, pH 7.8) for 15 min on ice. Total post-nuclear supernatants were then incubated in sample buffer (2% SDS, 10% glycerol, 0.1 M Tris–HCl, pH 6.8, 0.02% bromophenol blue), separated under reducing conditions on 15% SDS–polyacrylamide gels, transfered to nitrocellulose, and developed with a rabbit anti-CD3-ε antiserum (Dako) using an HRP-labeled goat anti-rabbit antiserum (Sigma) and the ECL detection protocol (Amersham).

### Antibodies and flow cytometry

Cells ($5\times10^5$) were stained with saturating levels of antibodies and $5–50\times10^3$ gated events were acquired using a Becton-Dickinson FACScan flow cytometer and analyzed with Lysis II software. Forward and side scatters were used to gate out dead cells. Biotinylated, FITC- or PE-conjugated antibodies against CD4 (GK1.5) and CD8α (53–6.7) were from Becton-Dickinson. Biotinylated, FITC- or PE-conjugated antibodies against CD3-ε (2C11), B220 (RA3-6B2), CD25(7D4), CD44 (Pgp-1), HSA (J11d), Thy1 (G7), TCR β (H57-597) and TCR δ (GL3) were purchased from Pharmingen. Biotinylated or FITC-conjugated antibodies against TCR β (H57-597), TCR δ (GL3), Mac-1 (M1/170), B220 (RA3-6B2) and Gr-1 (RA6-8c5) were from Caltag. Biotinylated antibodies were revealed with streptavidin-tricolor (Caltag).

### RNA-PCR amplification

Total RNA was prepared from thymocytes and NIH-3T3 fibroblastic cells using TRIzol™ (Gibco BRL) according to the manufacturer's protocol. Conversion to cDNA was done on 1 μg of total RNA using the Ready-to-Go™ T-primed first strand kit (Pharmacia). 1/20 of each reaction was used for PCR amplification. The Vβ5 (Vβ5 V), Vβ11 (Vβ11 V), Cβ2 (Cβ2 B), Vα8 (VαF3 V) and Dβ2 (Dβ2 5′) primers were as described in Anderson *et al.* (1992). The Cα (CII exon) primer was as described in Shimizu *et al.* (1992). The sequence of the other PCR primers used in these experiments were: CD3-ε a: 5′ CTGGGGCATCCTGTGC 3′; CD3-ε b: 5′ AGGGCTGGATCTGGG 3′; Vβ2: 5′ ATCCCTGGATGAGCTGGTAT 3′; Vα2: 5′ CTTCTAGGCC-TTCACCTAGCTGGT 3′; actin 5′: 5′ ACTCCGGTGACGGGGTCACC 3′; actin 3′: 5′ CACGATGGAGGGGCCGGACTC 3′:

The amplified products were analyzed on 1.5% agarose gel, transfered to nylon membrane (GeneScreen Plus, Dupont) and hybridized using either a 5′-kinased oligonucleotide (Cβ2 A; Anderson *et al.*, 1992) or a DNA fragment labeled by random priming (Cα-5′: 240 bp *Eco*RI–*Eco*RV fragment isolated from a mouse TCR-Cα cDNA; Malissen *et al.*, 1988).

### Detection of endogenous TCR rearrangement

Template genomic DNA (equivalent to $10^5$ cells per reaction) was prepared from thymocytes according to Köntgen *et al.* (1993). PCR-based analysis of β chain gene rearrangement was performed as described by Anderson *et al.* (1992). PCR-based analysis of TCR γ and TCR δ chain gene rearrangements used conditions previously described (Itohara *et al.*, 1993). Sequences of the Vδ, Vγ, Jδ and Jγ primers and oligonucleotide probes were as reported (Itohara *et al.*, 1993).

### Analysis of recombination substrate rearrangements

Three primers, denoted as 1, 2 and 3 in Figure 10, were used to amplify DNA extracted from thymocytes ($2\times10^3$ cells per reaction) and to analyze the status of the VDJ recombination substrate (Capone *et al.*, 1993). PCR amplification, gel electrophoresis and detection by Southern blot hybridization were as described by Capone *et al.* (1993). The sequences of the oligonucleotide probe and PCR primers used in these experiments were as described in Capone *et al.* (1993).

## Acknowledgements

We thank Pierre Golstein, Yujiro Tanaka, Rod Ceredig and Grace Ku for discussions and comments on the manuscript, Anne Wilson and Rob MacDonald for sharing unpublished data with us and for permission to cite them, Eugenia Spanopoulou for making available the RAG-$1^{-/-}$ mice, Anne Wilson and Nicole Brun for helpful discussions about FACS analysis. Delphine Guy-Grand for her advice on the isolation of gut intraepithelial lymphocytes, E.Termine for oligonucleotide synthesis, Gilles Warcollier and Michel Pontier for maintaining the mouse colony and Noëlle Guglietta for typing the manuscript. This work was supported by institutional grants from CNRS and INSERM, and by specific grants from the Association pour la Recherche Contre le Cancer and the Commission of the European Communities.

## References

Anderson,S.J., Abraham,K.M., Nakayama,T., Singer,A. and Perlmutter,M. (1992) Inhibition of T-cell receptor β-chain gene rearrangement by overexpression of the non-receptor protein tyrosine kinase $p56^{lck}$. *EMBO J.*, **11**, 4877–4886.

Artelt,P., Grannemann,R., Stocking,C., Friel,J., Bartsch,J. and Hauser,H. (1991) The prokaryotic neomycin-resistance-encoding gene acts as a transcriptional silencer in eukaryotic cells. *Gene*, **99**, 249–254.

Berget,S.M. (1995) Exon recognition in vertebrate splicing. *J. Biol. Chem.*, **270**, 2411–2414.

Bradley,A. (1987) Production and analysis of chimaeric mice. In Robertson,E.J. (ed.), *Teratocarcinomas and Embryonic Stem Cells—A Practical Approach.* IRL Press, Oxford, pp. 113–151.

Capone,M., Watrin,F., Fernex,C., Horvat,B., Krippl,B., Wu,L., Scollay,R. and Ferrier,P. (1993) TCRβ and TCRα gene enhancers confer tissue- and stage-specificity on V(D)J recombination events. *EMBO J.*, **12**, 4335–4346.

Clevers,H., Dunlap,S., Saito,H., Georgopoulos,K., Wileman,T. and Terhorst,C. (1988) Characterization and expression of the murine CD3-ε gene. *Proc. Natl Acad. Sci. USA*, **85**, 8623–8627.

Crompton,T., Moore,M., MacDonald,H.R. and Malissen,B. (1994) Double-negative thymocyte subsets in CD3ζ chain-deficient mice: absence of $HSA^+CD44^-CD25^-$cells. *Eur. J. Immunol.*, **25**, 1903–1907.

Dudley,E.C., Petrie,H.T., Shah,L.M., Owen,M.J. and Hayday,A.C. (1994) T cell receptor β chain gene rearrangement and selection during thymocyte development in adult mice. *Immunity*, **1**, 1–20.

Ehlich,A., Schaal,S., Gu,H., Kitamura,D., Muller,W. and Rajewsky,K. (1993) Immunoglobulin heavy and light chain genes rearrange independently at early stages of B cell development. *Cell*, **72**, 695–704.

Fairbairn,L.J., Cowling,G.J., Reipert,B.M. and Dexter,T.M. (1993) Suppression of apoptosis allows differentiation and development of a multipotent hemopoietic cell line in the absence of added growth factors. *Cell*, **74**, 823–832.

Godfrey,D.I. and Zlotnik,A. (1993) Control points in early T-cell development. *Immunol. Today*, **14**, 547–553.

Godfrey,D.I., Kennedy,J., Suda,T. and Zlotnik,A. (1993) A developmental pathway involving four phenotypically and functionally distinct subsets of $CD3^-CD4^-CD8^-$ triple-negative adult mouse thymocytes defined by CD44 and CD25 expression. *J. Immunol.*, **150**, 4244–4252.

Godfrey,D.I., Kennedy,J., Mombaerts,P., Tonegawa,S. and Zlotnik,A. (1994) Onset of TCR-β gene rearrangement and role of TCR-β expression during $CD3^-CD4^-CD8^-$ thymocyte differentiation. *J. Immunol.*, **152**, 4783–4792.

Groettrup,M., Baron,A., Griffiths,G., Palacios,R. and Von Boehmer,H. (1992) T cell receptor (TCR) β chain homodimers on the surface of immature but not mature α, γ and δ chain deficient T cell lines. *EMBO J.*, **11**, 2735–2746.

Groettrup,M., Ungewiss,K., Azogui,O., Palacios,R., Owen,M.J., Hayday,A.C. and Von Boehmer,H. (1993) A novel disulfide-linked heterodimer on pre-T cells consists of the T cell receptor β chain and a 33 kDa glycoprotein. *Cell*, **75**, 283–294.

Gu,H.G., Zou,Y.-R. and Rajewsky,K. (1993) Independent control of immunoglobulin switch recombination at individual switch regions evidenced through Cre–loxP-mediated gene targeting. *Cell*, **73**, 1155–1164.

Itohara,S., Mombaerts,P., Lafaille,J., Iacomini,J., Nelson,A., Clarke,A.R., Hooper,M.L., Farr,A. and Tonegawa,S. (1993) T cell receptor δ gene mutant mice: independent generation of αβ T cells and programmed rearrangements of γδ TCR genes. *Cell*, **72**, 337–348.

Jacobs,H., Vandeputte,D., Tolkamp,L., De Vries,E., Borst,J. and Berns,A. (1994) CD3 components at the surface of pro-T cells can mediate pre-T cell development *in vivo*. *Eur. J. Immunol.*, **24**, 934–939.

Kisielow,P. and Von Boehmer,H. (1995) Development and selection of T cells: facts and puzzles. *Adv. Immunol.*, **58**, 87–209.

Köntgen,F., Süss,G., Stewart,C., Steinmetz,M. and Bluethmann,H. (1993) Targeted disruption of the MHC class II Aa gene in C57BL/6 mice. *Int. Immunol.*, **5**, 957–964.

Letourneur,F., Mattei,M.-G. and Malissen,B. (1989) The mouse CD3-γ, -δ, an -ε genes reside within 50 kilobases on chromosome 9, whereas CD3-ζ maps to chromosome 1, band H. *Immunogenetics*, **29**, 265–268.

Levelt,C.N., Carsetti,R. and Eichmann,K. (1993a) Regulation of thymocyte development through CD3. II. Expression of T cell receptor β CD3ε and maturation to the $CD4^+8^+$ stage are highly correlated in individual thymocytes. *J. Exp. Med.*, **178**, 1867–1875.

Levelt,C.N., Mombaerts,P., Iglesias,A., Tonegawa,S. and Eichmann,K. (1993b) Restoration of early thymocyte differentiation in T-cell receptor β-chain-deficient mutant mice by transmembrane signaling through CD3ε. *Proc. Natl Acad. Sci. USA*, **90**, 11401–11405.

Levin,D.S., Anderson,S.J., Forbush,A.K. and Perlmutter,R.M. (1993) A dominant-negative transgene defines a role for $p56^{lck}$ in thymopoiesis. *EMBO J.*, **12**, 1671–1680.

Lewis,S.M. (1994) The mechanism of V(D)J joining: lessons from molecular, immunological, and comparative analyses. *Adv. Immunol.*, **56**, 27–150.

Liu,C.-P. *et al.* (1993) Abnormal T cell development in CD3-$\zeta^{-/-}$ mutant mice and identification of a novel T cell population in the intestine. *EMBO J.*, **12**, 4863–4875.

Love,P.E., Shores,E.W., Johnson,M.D., Tremblay,M.L., Lee,E.J., Grinberg,A., Huang,S.P., Singer,A. and Westphal,H. (1993) T cell development in mice that lack the ζ chain of the T cell antigen receptor complex. *Science*, **261**, 918–921.

Malissen,M., Trucy,J., Letourneur,F.,Rebai,N., Dunn,D.E., Fitch,F.W., Hood,L. and Malissen,B. (1988) A T cell clone expresses two T cell receptor α genes but uses one αβ heterodimer for all recognition and self-MHC restricted antigen recognition. *Cell*, **55**, 49–59.

Malissen,M., Trucy,J., Jouvin-Marche,E., Cazenave,P.-A., Scollay,R. and Malissen,B. (1992) Regulation of TCRα and β gene allelic exclusion during T-cell development. *Immunol. Today*, **13**, 315–322.

Malissen,M. *et al.* (1993) T cell development in mice lacking the CD3-ζ/η gene. *EMBO J.*, **12**, 4347–4355.

Manolios,N., Kemp,O. and Guo Li,Z. (1994) The T cell antigen receptor α and β chains interact via distinct regions with CD3 chains. *Eur. J. Immunol.* **24**, 84–92.

Mansour,S.L., Thomas,K.R. and Capecchi,M.R. (1988) Disruption of the proto-oncogene *int-2* in mouse embryo-derived stem cells: a general strategy for targeting mutations to non-selectable genes. *Nature*, **336**, 348–352.

McBurney,M.W., Sutherland,L.C., Adra,C.N., Leclair,B., Rudnicki,M.A. and Jardine,K. (1991) The mouse Pgk-1 gene promoter contains an upstream activator sequence. *Nucleic Acids Res.*, **19**, 5755–5761.

Mombaerts,P. *et al.* (1992) Mutations in T-cell antigen receptor genes α and β block thymocyte development at different stages. *Nature*, **360**, 225–231.

Mombaerts,P., Anderson,S.J., Perlmutter,R.M., Mak,T.W. and Tonegawa,S. (1994) An activated *lck* transgene promotes thymocyte development in RAG-1 mutant mice. *Immunity*, **1**, 261–267.

Pearse,M., Wu,L., Egerton,M., Wilson,A., Shortman,K. and Scollay,R. (1989) A murine early thymocyte developmental sequence is marked by transient expression of the interleukin 2 receptor. *Proc. Natl Acad. Sci. USA*, **86**, 1614–1618.

Punt,J.A., Kubo,R.T., Saito,T., Finkel,T.H., Kathiresan,S., Blank,K.J. and Hashimoto,Y. (1991) Surface expression a T cell receptor β (TCR-β) chain in the absence of TCR-α, -δ, and -γ proteins. *J. Exp. Med.*, **174**, 775–783.

Renard,V., Ardouin,L., Malissen,M., Milan,G., Lebastard,M., Gillet,A., Malissen,B. and Vivier,E. (1995) Normal development and function of natural killer cells in CD3-$\varepsilon^{\Delta 5/\Delta 5}$ mutant mice. *Proc. Natl Acad. Sci. USA*, in press.

Rolink,A., Karasuyama,H., Haasner,D., Grawunder,U., Martensson,I.L., Kudo,A. and Melchers,F. (1994) Two pathways of B-lymphocyte development in mouse bone marrow and the roles of surrogate L chain in this development. *Immunol. Rev.*, **137**, 185–201.

Rothenberg,E.V., Chen,D. and Diamond,R.A. (1993) Functional and phenotypic analysis of thymocytes in SCID mice. *J. Immunol.*, **151**, 3530–3546.

Saint-Ruf,C., Ungewiss,K., Groettrup,M., Bruno,L., Fehling,H.J. and Von Boehmer,H. (1994) Analysis and expression of a cloned pre-T cell receptor gene. *Science*, **266**, 1208–1212.

Shinkai,Y. and Alt,F.W. (1994) CD3ε-mediated signals rescue the development of $CD4^+CD8^+$ thymocytes in RAG-$2^{-/-}$ mice in the absence of TCR β chain expression. *Int. Immunol.*, **6**, 995–1001.

Shinkai,Y., Koyasu,S., Nakayama,K.I., Murphy,K.M., Loh,D.Y., Reinherz,E.L. and Alt,F.W. (1993) Restoration of T cell development in RAG-2-deficient mice by functional TCR transgenes. *Science*, **259**, 822–825.

Shinkai,Y., Ma,A., Cheng,H.L. and Alt,F.W. (1995) CD3ε and CD3δ cytoplasmic domains can independently generate signals for T cell development and function. *Immunity*, **2**, 401–411.

Shores,E.W., Sharrow,S.O., Uppenkamp,I. and Singer,A. (1990) T cell receptor-negative thymocytes from SCID mice can be induced to enter the CD4/CD8 differentiation pathway. *Eur. J. Immunol.*, **20**, 69–77.

Shores,E.W., Huang,K., Tran,T., Lee,E., Grinberg,A. and Love,P.E. (1994) Role of TCR ζ chain in T cell development and selection. *Science*, **266**, 1047–1050.

Spanopoulou,E. *et al.* (1994) Functional immunoglobulin transgenes guide ordered B-cell differentiation in Rag-1-deficient mice. *Genes Dev.*, **8**, 1030–1042.

Takeda,S., Zou,Y.R., Bluethmann,H., Kitamura,D., Muller,U. and Rajewsky,K. (1993) Deletion of the immunoglobulin κ chain intron enhancer abolishes κ chain gene rearrangement in *cis* but not L chain gene rearrangement in *trans*. *EMBO J.*, **12**, 2329–2336.

Wang,B., Biron,C., She,J., Higgins,K., Sunshine,M.J., Lacy,E.,

Lonberg,N. and Terhorst,C. (1994) A block in both early T lymphocyte and natural killer cell development in transgenic mice with high-copy numbers of the human CD3ε gene. *Proc. Natl Acad. Sci. USA*, **91**, 9402–9406.

Wang,B. *et al.* (1995) Over-expression of CD3ε transgenes blocks T lymphocyte development. *Int. Immunol.*, **7**, 435–448.

Wegener, A.M.K., Letourneur,F., Hoeveler,A., Brocker,T., Luton,F. and Malissen,B. (1992) The T cell receptor/CD3 complex is composed of at least two autonomous transduction modules. *Cell*, **68**, 83–95.

Wiest,D.L., Kearse,K.P., Shores,E.W. and Singer,A. (1994) Developmentally regulated expression of CD3 components independent of clonotypic T cell antigen receptor complexes on immature thymocytes. *J. Exp. Med.*, **180**, 1375–1382.

Wileman,T., Kane,L.P., Young,J., Carson,G.R. and Terhorst,C. (1993) Associations between subunit ectodomains promote T cell antigen receptor assembly and protect against degradation in the ER. *J. Cell. Biol.*, **122**, 67–78.

Wilson,A. and MacDonald,R. (1995) Expression of genes encoding the pre-T cell receptor and CD3 complex during thymus development. *Int. Immunol.*, in press.

Wilson,A., Held,W. and MacDonald,H.R. (1994) Two waves of recombinase gene expression in developing thymocytes. *J. Exp. Med.*, **179**, 1355–1360.

Wu,L., Scollay,R., Egerton,M., Pearse,M., Spangrude,G.J. and Shortman,K. (1991) CD4 expressed on earliest T-lineage precursor cells in the adult murine thymus. *Nature*, **349**, 71–74.

*Received on June 1, 1995; revised on June 29, 1995*